Application of a Micromechanical Model to Wave Propagation Through Nonlinear Rough Interfaces Under Stress

Anil Misra and Orestes Marangos
Department of Civil and Mechanical Engineering
University of Missouri-Kansas City
Kansas City, U.S.A.
misraa@umkc.edu

Abstract— **Imperfect interfaces between two rough solids are known to exhibit nonlinear, anisotropic behavior under static normal and shear stresses. We expect this nonlinear, anisotropic behavior to have a profound effect on wave propagation through such interfaces. A micromechanical methodology is applied to explicitly model the initial normal and shear stiffness behavior of interfaces. The calculated initial normal and shear stiffness are used to investigate plane wave propagation behavior through interfaces utilizing the imperfectly bonded interface model**

Keywords-interfaces; nonlinear; reflection coefficient; transmission coefficient; anisotropy

I. INTRODUCTION

The transmission of plane waves through rough interfaces, such as fractures or adhesive bonds, is of significance to the study of geophysical behavior of rock masses and other fractured materials. A number of researchers have investigated the transmission behavior of plane waves through rough surfaces in contact by treating them as imperfectly bonded interfaces represented by effective interface stiffness [see for example 1-3]. However, attempt has been made to relate the effective interface stiffness to the interface geometry and the mechanical properties of the material. Rough interfaces are highly inhomogeneous, and because of the surface roughness, the contact between surfaces is through local contact areas or asperities. The force-deformation behavior of an interface is determined by the behavior of asperity contacts. Consequently, the transmission of acoustic waves through interfaces is influenced by a variety of factors such as the frequency of the incident wave, the surface roughness, the mechanical properties of the material, and the existing normal and shear stress conditions.

The assumption which forms the basis of the wave propagation models based upon the concept of imperfectly bonded interfaces is that the wavelength is much larger than the asperity contact size and asperity contact separation. Under this assumption, the effective interface stiffness corresponding to interface length scales smaller than the size of wavelength should be considered. Thus, asperity contact stiffnesses at sub-wavelength scales may be averaged to obtain the overall interface stiffness. Asperities, at sub-wavelength scales, consist of different sizes and different orientations giving rise to variation in stiffness between different locations of the interface. Micromechanical approaches that explicitly include interface surface topography and incorporate material mechanical properties and intrinsic friction may be utilized to obtain the overall interface stiffness.

Recently, the author has developed a kinematically driven micromechanical methodology in which the stress-deformation behavior of an interface is obtained by considering the force-deformation behavior of the asperity contacts and the statistical description of surface topography [4-5]. The micromechanical methodology developed by the author extends other similar models [see 6 for a review] by using: (1) a directional distribution function of asperity contact orientations recognizing that the asperity contacts are not equally likely in all directions, and (2) an iterative procedure to obtain the asperity contact forces at each load increment, recognizing that the asperity contact force distribution is not known *a priori*. In the present paper, this micromechanical methodology for computing the overall interface stiffness is utilized along with the imperfectly bonded interface model to investigate how transmitted and reflected wave amplitudes are affected by the existing interface stress conditions.

In the subsequent discussion, we first briefly describe the essence of the kinematically driven micromechanical methodology. We then employ this model to study the behavior of wave transmission and reflection. We find that the amplitudes of the reflected and transmitted waves are significantly influenced by the interface stress conditions.

II. INTERFACE MICROMECHANICAL MODEL

We consider the micromechanical methodology wherein the stress-deformation behavior of an interface is obtained by considering the force-deformation behavior of the asperity contacts and the statistical description of the interface topography [5]. At the asperity contact-level, a local force-deformation relationship is defined that accounts for the elastic

deformation and inelastic sliding at the contact. As schematically depicted in Fig. 1, the stress-deformation relationship for an interface is then derived by utilizing: (1) the distribution functions of asperity heights and contact orientations, and (2) the overall kinematic constraints and equilibrium conditions.

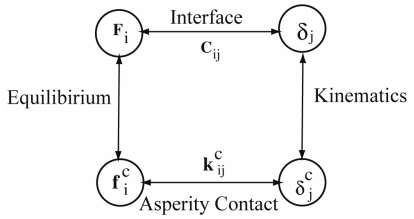

Figure 1. Schematic of the micromechanical modeling methodology.

A. Statistical Description of Interface

The interface geometry determines the orientations and the number of asperity contacts under a given loading condition. The composite topography of contacting surfaces, described via statistics of asperity contact heights, orientations, and curvatures, may be utilized for this purpose [7-8]. In this paper, the statistical distribution of asperity contact heights is described via gamma distributions, and that of asperity contact orientation via spherical harmonic expansions. It is usual to define the asperity contact height with reference to the highest peak of the composite topography such that, asperity height, r, represents the overlap of the interacting surfaces. The density function for asperity heights, *H(r)*, is given by a gamma distribution expressed as.

$$H(r)=\frac{r^{\alpha}\, e^{-r/\beta}}{\Gamma(\alpha+1)\beta^{\alpha+1}} \qquad (0<r<\infty,\ \alpha>-1,\ \beta>0) \qquad (1)$$

where α and β are parameters related to the mean and variance of the asperity heights as follows

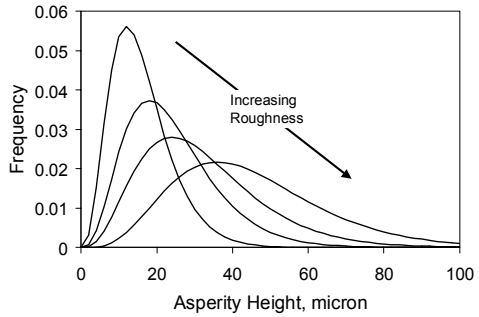

Figure 2. Asperity height distributions with varying surface roughness

$$\begin{aligned} &mean: && r_m=\beta(\alpha+1)\\ &variance: && r_\sigma^2=\beta^2(\alpha+1) \end{aligned} \qquad (2)$$

Parameter α is unit less while parameter β takes the unit of asperity height. Fig. 2 illustrates the distribution of asperity heights for surfaces with varying roughness. Surfaces that have smaller average asperity height and narrow distributions of asperity heights are considered to be relatively smoother. For an interface with *N* asperities per unit area, *N H(r) dr* denotes that number of asperity contacts in the interval represented by *r* and *r*+*dr*. Thus, the total number of asperity contacts, under a given loading condition, is given by

$$N_r=\int_0^r NH(r)dr \qquad (3)$$

where *r* represents the interface closure under a given loading.

The asperity contact orientation is defined by considering the inclination of the asperity contact normal with respect to that of the interface normal direction. As shown in Fig. 3, the orientation of an oblique asperity contact is defined by the azimuthal angle ϕ and the meridional angle θ, measured with respect to a Cartesian coordinate system in which direction 1 is normal to the interface.

A 3-dimensional density function utilizing spherical harmonics expansion in spherical polar coordinates that describes the concentrations of asperity contact orientations was introduced by [4-5]. For an interface with isotropic geometry, the density function, $\xi(\Omega)$, of asperity contact orientations distribution in the domain: $0\le\theta\le 2\pi/a,\ 0\le\phi\le 2\pi$, is given by

$$\xi(\Omega)=\frac{a\sin a\theta}{2\pi\sin\theta} \quad \left(0\le\theta\le\frac{\pi}{2a};\quad 0\le\phi\le 2\pi;\quad a\ge 1\right) \qquad (4)$$

where angles ϕ and θ are defined in Figure 3, Ω represents the solid angle formed by ϕ and θ, and parameter *a* determines the shape of the density function $\xi(\Omega)$. Thus, the product $N_r\xi(\Omega)d\Omega$ denotes the number of asperity contacts N_Ω in the interval represented by solid angles Ω and $\Omega+d\Omega$, that is

$$N_\Omega=N_r\xi(\Omega)d\Omega \qquad (5)$$

The density function in (10) has the ability to model surfaces with varying roughness. As discussed in [5], the asperity contacts for smooth interfaces have a greater tendency to concentrate in the direction normal to the interface than that for rough interfaces. It is noteworthy that, as parameter *a* increases, the contact distribution concentrates towards the direction normal to the interface. In particular, the density

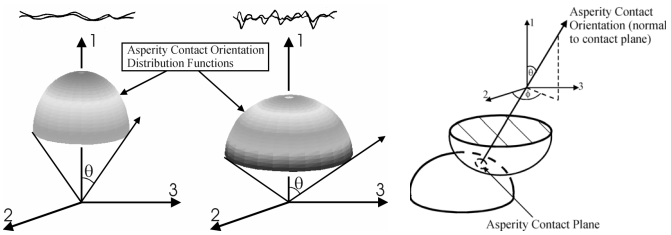

Figure 3. Depiction of asperity contact orientation distribution functions for smooth and rough interfaces.

function, $\xi(\Omega)$, behaves like a delta function in the limit $a \to \infty$ and yields an expectation $E[\theta] = 0$, which represents a concentrated contact orientation, normal to the interface of a perfectly smooth joint. In general, the parameter a, describes the extent of the asperity contacts in the meridional direction as well as the mean asperity contact orientation.

B. Interface Stress-Deformation Relationship

Considering the equilibrium of forces, the overall traction ΔF_i on the interface is obtained from the summation of the forces, Δf_i^c, developed at asperities, which for a large number of asperity contacts is written as the following integral:

$$\Delta F_i = N \int_r \int_\Omega \Delta f_i^c \, \xi(\Omega) H(r) d\Omega dr \tag{6}$$

where the traction ΔF_i is given as force per unit area since N is measured per unit area of an interface. The asperity contact forces, Δf_i^c, are related via the asperity contact stiffnesses, K_{ij}^c, to asperity contact displacement, $\Delta \delta_j^c$, as follows

$$\Delta f_i^c = K_{ij}^c \Delta \delta_j^c \tag{7}$$

The asperity contact stiffnesses, K_{ij}^c, generally depend upon the contact loading condition, such as the stiffness given by the Hertzian contact theory [9]. It is convenient to express the asperity stiffness tensor, K_{ij}^c, in terms of asperity stiffness that describes the behavior along the direction of normal and tangent to an asperity contact, such that

$$K_{ij}^c = K_n^c n_i^c n_j^c + K_s^c \left(s_i^c s_j^c + t_i^c t_j^c \right) \tag{8}$$

where K_n and K_s denote nonlinear asperity stiffness along the normal and tangential direction of the asperity. The unit vector **n** is normal to the asperity contact surface and vectors **s** and **t** are arbitrarily chosen on the plane tangential to the asperity contact surface, such that **nst** forms a local Cartesian coordinate system. It is noted that the stiffness term that cross-link normal and shear behavior are assumed to be negligible in accordance with the theories for contact of smooth non-conforming bodies. The Amonton-Coulomb's friction law, expressed by the following inequality governs the sliding at an asperity contact:

$$f_i^c q_i^c \le 0 \text{ where } q_i^c = \zeta_i^c + \mu n_i^c \tag{9}$$

ζ_i^c is a unit vector in the sliding direction, μ is the asperity friction coefficient and n_i^c is a unit vector outwardly normal to the asperity contact. Under a given loading condition, an asperity contact may be sliding, or separated. Appropriately accounting for the asperity contact forces, and adopting the kinematic assumption that relative motion at an asperity, $\Delta \delta_j^c$, is same as the relative motion of the interface, $\Delta \delta_j$, the overall traction, ΔF_i, may be written as:

$$\Delta F_i = C_{ij} \Delta \delta_j \tag{10}$$

where interface stiffness tensor is denoted by, C_{ij}. The domain of sliding and separated asperity contacts is not always known a priori [5]. Moreover, the sliding domain evolves with loading. In addition, new asperity contacts are formed and existing contacts lost as the interface is sheared. Numerically, the asperity separation may be detected by examining the total relative displacement in the normal direction of an asperity contact. Consequently, an incremental interface stress-displacement relationship is obtained by numerically integrating the following equations for each loading step:

$$C_{ij} = N \int_0^r \int_0^{2\pi} \int_0^{\pi/2a} K_{ij}^c \, \xi(\phi,\theta) \sin\theta \, d\theta \, d\phi H(r) \, dr \tag{11}$$

where $\xi(\phi,\theta)$ is the asperity contact orientation distribution given by (10), and H(r) is asperity height distribution given by (7), $r = r_o + \delta_l$, r_o is the initial closure at $\delta_l = 0$. As a result, shear stress – shear displacement relationships may be obtained, as illustrated in Fig. 4. The corresponding evolution of the interface stiffness is also shown in Fig. 4. As seen, at zero shear stress, the interface shear stiffness is isotropic, that is $C_{22} = C_{33}$. However, as the shear stresses are increased, the two shear stiffnesses deviate considerably leading to induced anisotropy. Moreover, the coupling term, C_{13}, between the normal stress and the shear displacement along the loading direction (3-axis) becomes non-zero and evolves with shear loading.

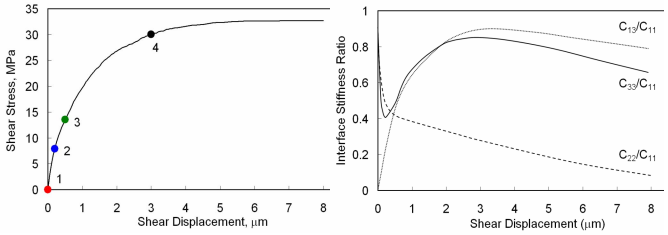

Figure 4. Shear stress-shear displacement behavior and evolution of interface stiffness.

III. Wave Propagation through Interface

The micromechanical model described above is applied to investigate wave propagation through rough interfaces based upon the imperfectly bonded interface model, also known as linear slip or displacement discontinuity approach [1-3]. We give a brief description of the imperfectly bonded interface methodology in order to define the appropriate quantities.

A. Imperfectly Bonded Interface

For convenience, we choose a coordinate system, such that the direction of incident wave propagation is within the 1-3 plane shown in Fig. 3. At an imperfect interface between two media, tractions at upper medium A and lower medium B are continuous and displacements are discontinuous, which lead to the following equations where n=0-3 and n=4-6 are the wave modes in the incident and transmitting media, respectively.

$$\sum_{n=0}^{3}\sigma_{i1}^{(n)A} = \sum_{n=4}^{6}\sigma_{i1}^{(n)B} \tag{12}$$

$$\sum_{n=4}^{6}\sigma_{i1}^{(n)B} = \left(\sum_{n=4}^{6}\Delta u_j^{(n)} - \sum_{n=0}^{3}\Delta u_j^{(n)}\right)C_{ij} \tag{13}$$

We note that the interface overall traction, ΔF_i, and the relative motion of the interface, $\Delta\delta_j$, are given as

$$\Delta F_i = \sum_{n=4}^{6}\sigma_{i1}^{(n)B}, \Delta\delta_j = \sum_{n=4}^{6}\Delta u_j^{(n)} - \sum_{n=0}^{3}\Delta u_j^{(n)} \tag{14}$$

Equations (12) and (13) may be combined to obtain the amplitudes of the reflected and transmitted P and S waves for the interface as follows

$$\begin{bmatrix}[A] & [B]\\ [D] & [E]\end{bmatrix}\begin{Bmatrix}\{R\}\\ \{T\}\end{Bmatrix} = \begin{Bmatrix}\{C\}\\ \{F\}\end{Bmatrix} \tag{15}$$

where the transfer matrices [A], [B], [D] and [E] are a function of elastic constants of upper and lower media, and the nonlinear, stress-dependent interface stiffnesses derived from the micromechanical model described in section II. Thus, the solution of (15) generates complex valued reflection, $\{R\}$, and transmission, $\{T\}$, coefficients which are related to interface stresses and roughness.

B. Results for Reflection and Transmission at Interfaces

We investigate the reflection and transmission of normally incident shear wave (propagating along 1-axis) to illustrate the effects of nonlinear, stress-dependent interface stiffnesses. In Fig. 5, we plot, in polar coordinates, the reflection and transmission coefficients at several shear stress conditions of the interface whose stress-displacement behavior is given in Fig. 4. Four shear stress levels are considered as denoted by different colored filled circles in Fig. 4. The polar plots correspond to the incident shear-wave's polarization direction given by the azimuthal angle, ϕ. For instance, ϕ=0 corresponds to the polarization direction along the 3-axis. At zero shear stress, denoted by the red curve in Fig. 5, normally incident shear wave does not suffer any mode conversion, and this is true for all polarization directions of the incident shear wave.

As the shear stresses are increased, we observe that the normally incident shear wave suffers mode conversion to transmitted and reflected P and SH waves. Similar mode conversion has been observed experimentally [10]. When the incident shear wave is polarized along the 3 axis, the SH wave reflected and transmitted amplitudes are zero, however, the corresponding mode converted P-wave amplitude is non-zero. When the direction of polarization of the incident shear wave is along the 2 axis, then both the mode converted SH and P wave amplitudes are zero. For any other incident shear wave polarization direction, the amplitudes of the mode converted waves are non-zero. Furthermore, we observe that the reflected and the transmitted of the mode converted waves are equal in amplitude. It is noteworthy that the amplitudes of the reflected and transmitted waves are dependent upon the direction of polarization. It is also evident that the transmitted and reflected wave amplitudes are critically dependent upon the state of shear stress. For instance, reflectance and transmittance behavior of the SV wave amplitudes with the azimuthal angle ϕ

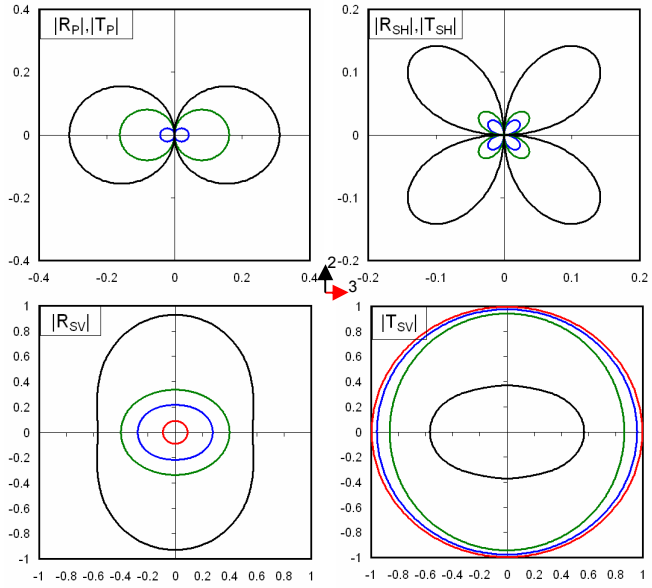

Figure 5. Reflection and transmission coefficients for normal incidence of SV waves showing mode conversion.

changes dramatically from red to blue to green to black curves in Fig. 5.

REFERENCES

[1] Kendal, K. and Tabor, D. An ultrasonic study of area of contact between stationary and sliding surfaces. Proc. R. Soc. London, vol. A323, pp. 321-340, 1971.

[2] Rokhlin, S.I. and Wang, Y.J. Analysis of boundary conditions for elastic wave interaction with an interface between two solids. J. Acoust. Soc Am., vol 89, pp. 503-515, 1991.

[3] Schoenberg, M. Elastic wave behavior across linear slip interfaces. J. Acoust. Soc Am., vol. 68, pp. 1516-1521, 1980.

[4] Misra, A. Mechanistic model for contact between rough surfaces, J. Eng. Mech., vol. 123, pp. 475-484, 1997.

[5] Misra, A. Micromechanical model for anisotropic rock joints, J Geophys Res, vol. 104, pp. 23,175-23,187, 1999.

[6] Yoshioka, N. A review of the micromechanical approach to the physics of contacting surfaces, Tectonophysics, vol. 277, pp. 29-40, 1997.

[7] Adler, RJ, Firman, D. A non-Gaussian model for random surfaces, Phil Trans Royal Soc London, vo.A303, pp.433-462, 1981.

[8] Nayak, P.R., Random process model of rough surfaces, J. Lubr. Technol., vol. 93, 398-407, 1971.

[9] Johnson, KL, Contact Mechanics, London, UK: Cambridge University Press; 1985.

[10] Nakagawa, S., Nihei, K.T., Myer, L.R. Shear-induced conversion of seismic waves across single fractures.Int. J. Rock Mech.Min Sci., vol. 37, pp. 203-218, 2000.